A-1-2

Extended Abstracts of the 2013 International Conference on Solid State Devices and Materials, Fukuoka, 2013, pp526-527

Abnormal Cell-to-Cell Interference of NAND Flash Memory

Yong Jun Kim[1], Jun Geun Kang[1], Byungin Lee[2], Gyu-Seog Cho[2], Sung-Kye Park[2], and Woo Young Choi[1]

[1]Department of Electronic Engineering, Sogang University, 35 Baekbeom-ro, Mapo-gu, Seoul 121-742, Korea

[2]SK Hynix, 2019 Gyeongchung-daero Bubal-eub Icheon-si Gyeonggi-do, Korea

Phone: +82-2-715-8467 Fax: +82-2-715-8467 E-mail: tlwmfjtnl@hanmail.net

Abstract

Abnormal increase of cell-to-cell interference in 2y-nm NAND flash memory has been discussed. When a p-type floating gate (FG) and control gate (CG) are introduced, the depletion region variation depending on operation modes in the FG and CG affects CG-to-FG coupling capacitance and threshold voltage variation. It has also been found that there is a symmetry between n-type FG/CG and p-type FG/CG flash memory in terms of cell-to-cell interference.

1. Introduction

It is well-known that cell-to-cell interference increases as NAND flash memory cells are scaled down. It is because cell-to-cell parasitic capacitance increases as the separation gap between adjacent cells decreases [1]-[3]. Because cell-to-cell interference causes threshold voltage variation (ΔV_T) of a victim cell during read operation, it needs to be simulated by including all the capacitance components surrounding a victim cell for the improvement of accuracy. Recently, NAND flash memory cells whose floating gate (FG) and control gate (CG) are doped p-type have been introduced [4], [5]. This paper is contributed to abnormal cell-to-cell interference of p-type FG/CG cells while n-type FG/CG case has already been reported elsewhere [1]. In this paper, it is found that cell-to-cell interference of n- and p-type FG/CG shows symmetrical relationship determined by the depletion region variation (ΔW_{dep}) of FG/CG.

2. Simulation and Results

Three-dimensional device simulation has been performed by using commercial device simulators. Fig. 1a shows the simulated 1x2 NAND flash array. Fig. 1b shows its cross-sectional view in the word-line direction. The simulated NAND flash cell has a gate length of 2y-nm. For p-type FG/CG cells, p-type polysilicon has been used whose work function is 5.17eV. For comparison, n-type FG/CG cells have also been simulated which use n-type polysilicon whose work function is 4.05eV. The V_T variation of a victim cell has been extracted when a neighbor cell is in erase and program state. Polysilicon depletion and parasitic capacitance have been included in simulation for higher accuracy. Fig. 2 shows the abnormal cell-to-cell interference of n- and p-type FG/CG NAND flash arrays. As shown in Fig. 2, there is a symmetrical relationship between the n-type and p-type FG/CG case. It is because p-type FG/CG cells show the ΔW_{dep} trend opposite to n-type FG/CG cells depending on the state of victim and neighbor cells. The ΔW_{dep} variation of p-type FG/CG cells has been discussed.

Fig. 3 shows the ΔW_{dep} of a CG as a victim cell is changed from the weak erase state (Fig. 3a) to the strong erase state (Fig. 3b). The variation becomes smaller as the FG of a victim cell has more positive charge. It is because the depletion region of a CG is maximized regardless of the victim cell state when a neighbor cell is the erase state. However, the depletion region of a CG becomes larger as a victim cell approach the strong erase state when a neighbor cell is in the program state. It makes ΔV_T decrease.

Fig. 4 shows the ΔW_{dep} of a FG as the victim cell state is changed from weak program (Fig. 4a) to strong program (Fig. 4b). The variation becomes larger as the FG of a victim cell has more negative charge. Because the voltage applied to a CG is the same as the V_T of a victim cell, CG voltage increases as the victim cell becomes programmed more strongly. The depletion region of a FG also increases as a neighbor cell is changed from the program state to the erase state at the increased CG voltage. Thus, ΔV_T increases.

Fig. 5 shows the cause of abnormal cell-to-cell interference which is determined by the ΔW_{dep} of a CG as the victim cell state is changed from weak program (Fig. 5a) to weak erase (Fig. 5b). The variation becomes larger as the FG of a victim cell has less positive charge. It is because the CG depletion region is minimized regardless of the victim cell state when a neighbor cell is in the program state. However, the region becomes larger as a victim cell approaches the weak erase state when a neighbor cell is in the erase state. It makes ΔV_T decrease. The ΔW_{dep} of a p-type FG/CG cell shows the trend opposite to that of an n-type FG/CG cell [1].

A reasonable solution to abnormal cell-to-cell interference is to increase the doping concentration of a FG/CG. Fig. 6 and 7 show that cell-to-cell interference is suppressed as the doping concentration of a FG/CG increases. In the case of an n-type FG/CG cell, a highly doped CG reduces ΔV_T when a victim cell is in the program state while a highly doped FG reduces ΔV_T when a victim cell is in the erase state. On the other hand, a p-type FG/CG cell shows an opposite trend compared with an n-type FG/CG cell. Thus, as shown Fig. 8, a highly doped n- and p-type FG/CG cell can reduce abnormal cell-to-cell interference.

3. Summary

The symmetrical cell-to-cell interference trend has been observed between the n- and p-type FG/CG NAND flash array. The symmetrically abnormal cell-to-cell interference is caused by CG to FG coupling capacitance variation. Also, the variation is caused by the ΔW_{dep} of a FG/CG of a victim cell as the state of a neighbor cell is changed from erase to program. The interference can be suppressed by increasing the doping concentration of a highly doped n- and p-type FG/CG.

Acknowledgements

This work was supported in part by the NRF of Korea funded by the MSIP under Grant 2013-027714 (Mid-Career Researcher Program), in part by the NIPA funded by the MSIP under Grant NIPA-2013-H0301-13-1007 (University ITRC Support Program), in part by the KEIT funded by the MOTIE under Grant 10039174 (IT R&D Program) and in part by the Sogang University Research Grant of 2012.

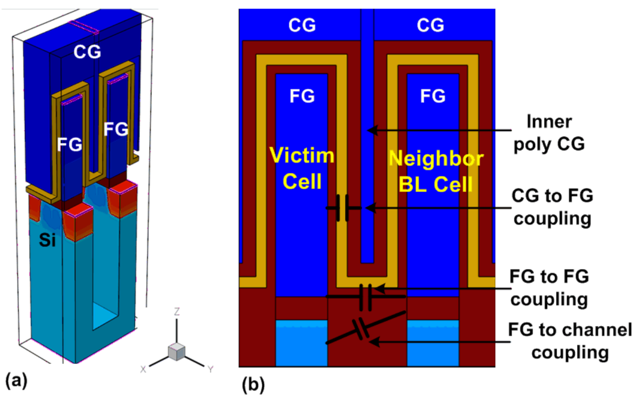

Fig. 1. (a) 3D structure of NAND flash array. (b) Cross-section of NAND flash and capacitances of a victim cell channel and floating gate.

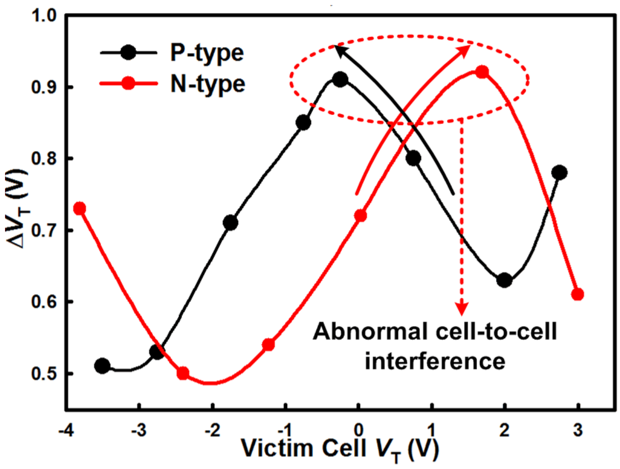

Fig. 2. Symmetrical abnormal cell-to-cell interference of an n- and p-type FG/CG cell.

References

[1] E. Kwon *et al.*, *Proc. Int. Conf. SISPAD*, pp. 207-210, 2011. [2] M. Park *et al.*, *IEEE Elec. Dev. Lett.,* vol. 30, no. 2, pp. 174-177, Feb. 2009. [3] J.-D. Lee *et al.*, *IEEE Elec. Dev. Lett.,* vol. 23, no. 5, pp. 264-266, May 2002. [4] C. H. Lee *et al.*, *IEEE Int. IMW Conf.*, pp. 1-4, 2012. [5] C. Shen *et al.*, *IEEE Trans. Elec. Dev.* vol. 54, no. 8, pp. 1910-1917, Aug. 2007.

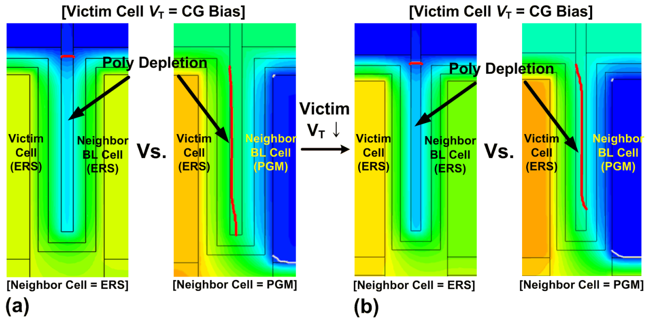

Fig. 3. CG depletion region variation (a) when a victim cell is weakly erased and (b) when a victim cell is strongly erased.

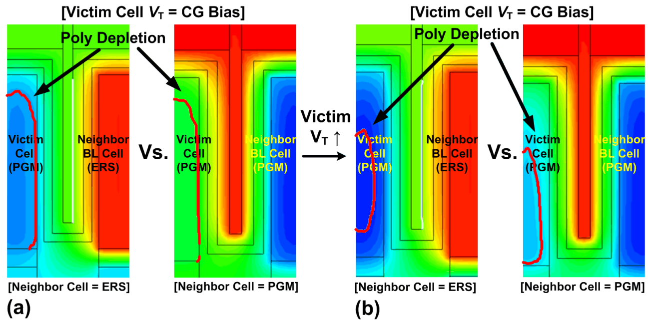

Fig. 4. FG depletion region variation (a) when a victim cell is weakly programmed and (b) when a victim cell is strongly programmed.

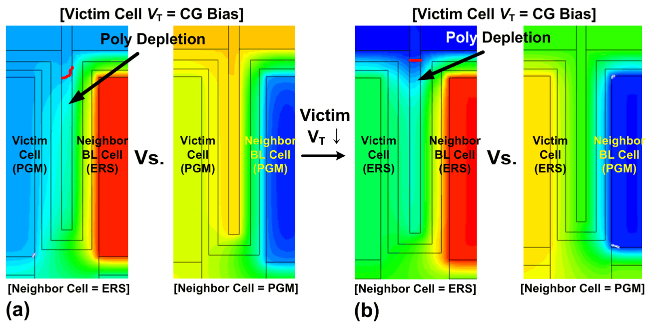

Fig. 5. CG depletion region variation (a) when a victim cell is weakly programmed and (b) when a victim cell state is weakly erased.

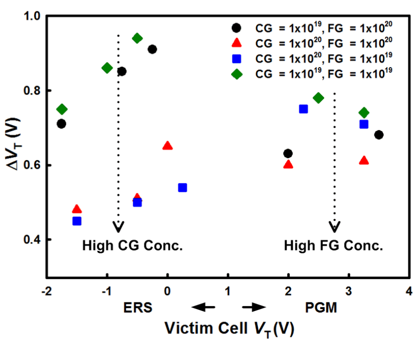

Fig. 6. Cell-to-cell interference of an n-type NAND flash with the variation of the doping concentration of a FG/CG.

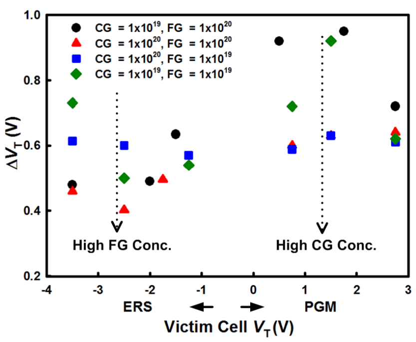

Fig. 7. Cell-to-cell interference of a p-type NAND flash with the variation of the doping concentration of a FG/CG.

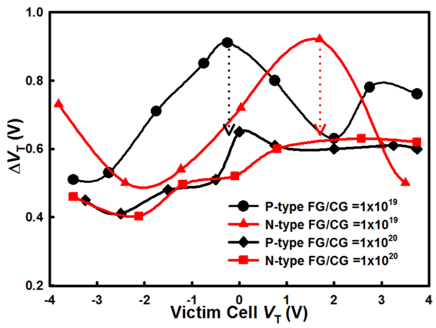

Fig. 8. Cell-to-cell interference comparison between an n- and p-type NAND flash memory array.